Emergence of robustness in networks of networks

Kevin Roth,[1,2] Flaviano Morone,[1] Byungjoon Min,[1] and Hernán A. Makse[1,*]
[1]*Levich Institute and Physics Department, City College of New York, New York, New York 10031, USA*
[2]*Theoretical Physics, ETH Zürich, 8093 Zürich, Switzerland*
(Received 27 April 2016; revised manuscript received 3 March 2017; published 30 June 2017)

A model of interdependent networks of networks (NONs) was introduced recently [Proc. Natl. Acad. Sci. (USA) **114**, 3849 (2017)] in the context of brain activation to identify the neural collective influencers in the brain NON. Here we investigate the emergence of robustness in such a model, and we develop an approach to derive an exact expression for the random percolation transition in Erdös-Rényi NONs of this kind. Analytical calculations are in agreement with numerical simulations, and highlight the robustness of the NON against random node failures, which thus presents a new robust universality class of NONs. The key aspect of this robust NON model is that a node can be activated even if it does not belong to the giant mutually connected component, thus allowing the NON to be built from below the percolation threshold, which is not possible in previous models of interdependent networks. Interestingly, the phase diagram of the model unveils particular patterns of interconnectivity for which the NON is most vulnerable, thereby marking the boundary above which the robustness of the system improves with increasing dependency connections.

DOI: 10.1103/PhysRevE.95.062308

I. INTRODUCTION

Many biological, social, and technological systems are composed of multiple, if not vast numbers of, interacting elements. In a stylized representation, each element is portrayed as a node and the interactions among nodes as mutual links, thus forming what is called a network [1]. A finer description further isolates several subnetworks, each of them performing a different function. These subnetworks are, in turn, integrated to form a larger aggregate referred to as a network of networks (NON). A compelling problem is how to define the interdependencies between networks, specifically how the functioning of nodes in one network controls the functioning of nodes in other networks [2–6].

Current models of interdependent NONs inspired by the power grid represent such dependencies across networks through prohibitively fragile couplings [2,3], such that the random failure of few nodes gives rise to a catastrophic cascading collapse of the entire NON. The reason for such a catastrophic vulnerability lies in a global rule of interconnectivity between networks: nodes are activated only when they are part of the mutually connected giant component. Thus, a single node has to carry the information about the entire extensive giant component, and small isolated activated clusters are not allowed as the node's activity depends globally on the connectivity of the whole NON. This global dependency for functionality in the network leads to discontinuous sudden transitions from a connected phase to a disconnected phase, which is, however, not reversible, i.e., the NON cannot be built from below the percolation transition.

Many real-life systems, however, exhibit high resilience against malfunctioning. The prototypical example of such robust modular architectures is the brain, which thus cannot fit in catastrophic NON models [6]. To overcome the fragility of current NON models, we recently introduced a model of interdependencies in NONs in which dependency or control links do not need to be part of the global giant connected component G for their proper functioning [7]. Our model is inspired by the phenomenon of top-down control in brain activation between neural networks connected by weak links [8–10]. The key point in our model is that a node can be activated even if it does not belong to G. We thus separate the (local) notion of activity from the (global) concept of the giant connected component, allowing us to build the NON from below the percolation threshold, which is not possible in previous models of interdependent networks [2,3]. As a result, dependencies, which are now called controlling links in the robust NON, do not lead to cascades of failures, and the robust model exhibits second-order transitions at the percolation threshold. Interestingly, similar ideas have been put forward in a NON model in Ref. [11].

We initially [7] studied the impact of rare events, i.e., nonrandom *optimal percolation* [12], on this NON, allowing us to identify the neural collective influencers (NCIs) in the brain [7], with application to neurological disorders. These NCIs are the minimal number of nodes in the NON, that upon removal lead to the destruction of the mutually giant connected component, which is a generalization of the optimal percolation process presented in [12,13] from single networks to NONs.

Here we investigate the robustness of this NON model with respect to typical node failures, i.e., *random percolation*. More precisely, we develop an approach to derive an analytical expression for the random percolation phase diagram in Erdös-Rényi (ER) NONs and ER multiplex networks. Our calculations unveil the conditions responsible for the emergence of robustness, and predict the critical fraction of interdependencies above which the system becomes more robust with an increase in dependency connections, thus presenting a new robust universality class.

II. DEFINITION OF CONTROL LINKS

Consider N nodes in a NON composed of several interdependent modules (Fig. 1). We distinguish the roles

*hmakse@lev.ccny.cuny.edu

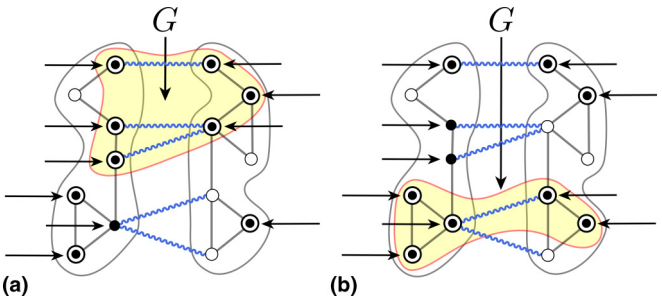

FIG. 1. Robust interdependent 2-NON. Intramodule links (black) represent connectivity, while intermodule links (wiggly blue lines) express mutual control. The occupation variable n_i specifies whether a node is present ($n_i = 1$; indicated by an $\longrightarrow$ to guide the eye) or removed ($n_i = 0$; no arrow). The activation state σ_i, defined through intermodule control links, indicates whether a node is activated ($\sigma_i = 1$; ⦿) or inactivated ($\sigma_i = 0$; ○ and •). Nodes can be activated even if they do not belong to the giant connected activated component G, and control links do not need to be part of G for their proper functioning [see, for instance, the topmost pair of nodes in (b)]. A node can be part of G without being part of the largest connected activated component in its own module [consider, for instance, the top-left node in (a)]. Legend: ⦿ $\sigma_i = 1$; • $n_i = 1, \sigma_i = 0$; ○ $n_i = 0, \sigma_i = 0$.

of intramodule connectivity links, connecting nodes within a module, and intermodule control or dependency links, connecting nodes across modules: while the former only represent whether or not two nodes are connected, the latter additionally express mutual control. Every node i has k_i^{conn} connectivity links and k_i^{ctr} control connections, respectively referred to as node i's connectivity-degree and control-degree.

Each node can be present or removed, and, if present, it can be activated or inactivated. We introduce the binary occupation variable $n_i = 1,0$ to specify whether node i is present ($n_i = 1$) or removed ($n_i = 0$). By virtue of intermodule control or dependency connections, the functioning of a node in one module controls or depends on the functioning of nodes in other modules. To conceptualize this form of control, we introduce the activation state σ_i, taking values $\sigma_i = 1$ if node i is activated and $\sigma_i = 0$ if not. A node i with one or more intermodule control links ($k_i^{\text{ctr}} \geqslant 1$) is activated ($\sigma_i = 1$) if and only if it is present ($n_i = 1$) and at least one of its intermodule neighbors j is also present ($n_j = 1$), otherwise it is not activated ($\sigma_i = 0$). In other words, a node with one or several intermodule dependencies is inactivated when the last of its intermodule neighbors is removed.

The rationale for this control rule is that the activation ($\sigma_i = \sigma_j = 1$) of two nodes connected by, for instance, one interlink occurs only when both nodes are occupied ($n_i = n_j = 1$). If just one of them is unoccupied, say $n_j = 0$, then both nodes become inactive. Thus, $\sigma_i = 0$ even though $n_i = 1$, and we say that j exerts a control over i. This rule models the way neurons control the activation of other neurons in distant brain modules (via fibers through the white matter) in a process known as top-down influence in sensory processing [10]. Mathematically, σ_i is defined as

$$\sigma_i = n_i \left[1 - \prod_{j \in \mathcal{F}(i)} (1 - n_j) \right] \quad \text{for } k_i^{\text{ctr}} \geqslant 1, \tag{1}$$

where $\mathcal{F}(i)$ denotes the set of nodes connected to i via a control link. Conceptually, the control links define a mapping from the configuration of occupation variables $\vec{n} \equiv (n_1, \ldots, n_N)$ to the configuration of activated states $\vec{\sigma} \equiv (\sigma_1, \ldots, \sigma_N)$, as given by Eq. (1).

Not all nodes participate in the control of other nodes via dependencies, however, i.e., a certain fraction of them does not establish intermodule control connections. If a node does not have intermodule links, it activates as long as it is present:

$$\sigma_i = n_i \quad \text{for } k_i^{\text{ctr}} = 0. \tag{2}$$

This property also guarantees that we recover the single-network case for vanishing intermodule connections ($\langle k_i^{\text{ctr}} \rangle = 0$), i.e., when considering the limiting case of one isolated module only.

The above control rule can alternatively be expressed by the McCulloch-Pitts model of neural activation [14]:

$$\sigma_i = 0 \qquad \text{for direct inactivation,} \tag{3}$$

$$\sigma_i = \Theta\left(\sum_{j \in \mathcal{F}(i)} \sigma_j \right) \qquad \text{for indirect inactivation,} \tag{4}$$

where a node can be inactivated directly (in which case we set $\sigma_i = 0$) or it can be inactivated indirectly as a result of a lack of input from its inactivated neighbors. The sum over $\mathcal{F}(i)$ in the second equation reflects the integration of incoming activity from nodes j in other modules connected to node i via control links. The threshold operation via the Heaviside step function Θ indicates that a minimum of incoming activity is needed for activation to propagate.

When a fraction of nodes is removed, the NON breaks into isolated components of activated nodes. In this work, we focus on the *largest (giant) mutually connected activated component* G, which encodes global properties of the system. In contrast to previous NON models [2,3], in our model a node can be activated even if it does not belong to G (see Fig. 1). Indeed, the activation of a node, given by Eq. (1), is not tied to its membership in the giant component. Therefore, a node can be part of G without being part of the largest connected activated component in its own module [consider, for instance, the top left node in Fig. 1(a)]. As a consequence, controlling dependencies in the NON do not lead to cascades of failures, which ultimately explains the robustness of our NON model. In the model of Refs. [2,3], on the other hand, a node can be activated (therein termed "functional") if and only if it belongs to the largest connected component of its own module, and (for the case when it has intermodule dependency links) its intermodule neighbors also belong to the giant component within their module. Indeed, in Refs. [2,3] the propagation of failures is not local as in Eq. (1), implying that the failure of a single node may catastrophically destroy the NON.

To quantify the robustness of our NON, we measure the impact of node failures $n_i = 0$ on the size of G [2–4]. More precisely, we calculate G under random configurations $\vec{n}$, sampled from a flat distribution with a given fraction $q \equiv 1 - \sum_{i=1}^{N} n_i / N$ of removed nodes, and we show that G remains sizable even for high values of q. In practice, starting from $q = 0$, we compute $G(q)$ while progressively

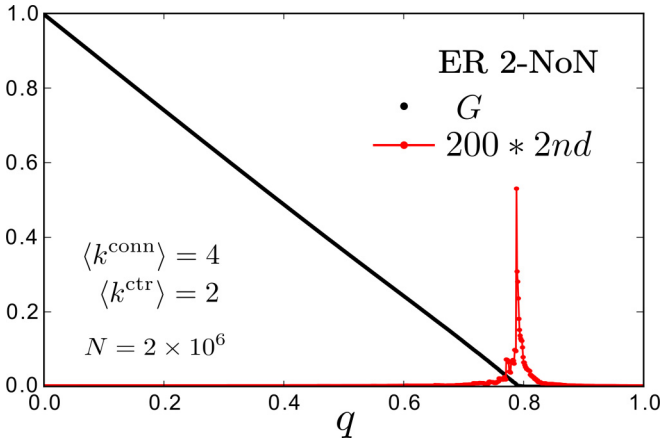

FIG. 2. Percolation transition. Fraction of nodes in G (black dots) and 200 $*$ size of the second largest connected activated component (red dots) as a function of q for an ER 2-NON with $\langle k^{\rm conn}\rangle = 4$, $\langle k^{\rm ctr}\rangle = 2$, and $N = 2 \times 10^6$. The percolation threshold q_c denotes the critical fraction of randomly removed nodes at which $G(q_c) = 0$ collapses. The numerical value $q_c^{\rm num} = 0.788$ is obtained at the peak of the second largest activated component. The percolation transition, separating the phases $G > 0$ and $G = 0$, is of second order in the robust NON.

increasing the fraction q of randomly removed nodes. The robustness of the NON is then formally characterized by the critical fraction q_c, the percolation threshold, at which the giant connected activated component collapses, $G(q_c) = 0$ [2,3]. Consequently, NON models with high q_c (ideally close to 1) are robust, whereas those with low q_c are considered fragile. A plot of $G(q)$ for an ER 2-NON is shown in Fig. 2.

III. MESSAGE PASSING

From a practitioner's point of view, the size of G in a particular NON realization can be computed using a breadth-first search strategy [1], which consecutively identifies activated neighbors (and neighbors of neighbors, etc.) until all nodes have been assigned the label of the corresponding cluster to which they belong.

In the limit of large network size ($N \to \infty$), the problem of calculating G can also be solved using a message-passing approach [4,12,15], which provides exact solutions on a locally treelike NON, containing a small number of short loops [15]. This includes the thermodynamic limit of Erdös-Rényi and scale-free random graphs as well as the configuration model (the maximally random graphs generated from a given degree distribution), which contain loops whose typical length grows logarithmically with the system size [16].

The virtue of the message-passing approach lies in the fact that it allows us to make statements about the typical percolation behavior of large networks through the computation of ensemble averages, i.e., by averaging the message-passing equations over all realizations of randomness inherent in the percolation process [15].

In principle, message passing works like this: each node receives messages from its neighbors containing information about their membership in G. Based on what they receive, the nodes then send further messages until everyone eventually agrees on who belongs to G. In practice, we need to derive a self-consistent system of equations that specifies for each node how the message to be sent is computed from the incoming messages [17]. To that end, we introduce two types of messages: $\rho_{i\to j}$ running along an intramodule connectivity link and $\varphi_{i\to j}$ running along an intermodule control link. Formally, we denote $\rho_{i\to j} \equiv$ *probability that node i is connected to G other than via intramodule neighbor j*, and $\varphi_{i\to j} \equiv$ *probability that node i is connected to G other than via intermodule neighbor j*. The binary nature of the occupation variables and the activation states constrains the messages to take values $\rho_{i\to j}, \varphi_{i\to j} \in \{0,1\}$.

The self-consistent system of message-passing equations corresponding to our model can then be derived as follows. A node can only send nonzero information if it is activated, hence the messages must be proportional to σ_i. Assuming node i is activated, it can send a nonzero intramodule message $\rho_{i\to j}$ to node j if and only if it receives a nonzero message by at least one of its intramodule neighbors other than j *or* one of its intermodule neighbors. Similarly, we can consider the message $\varphi_{i\to j}$ along an intermodule link. Assuming node i is activated, it can send a nonzero message to node j if it receives a nonzero message by at least one of its intramodule neighbors *or* one of its intermodule neighbors other than j. Thus, the self-consistent system of message-passing equations is given by

$$\rho_{i\to j} = \sigma_i \left[1 - \prod_{k\in\mathcal{S}(i)\setminus j} (1-\rho_{k\to i}) \prod_{k\in\mathcal{F}(i)} (1-\varphi_{k\to i}) \right], \quad (5)$$

$$\varphi_{i\to j} = \sigma_i \left[1 - \prod_{k\in\mathcal{S}(i)} (1-\rho_{k\to i}) \prod_{k\in\mathcal{F}(i)\setminus j} (1-\varphi_{k\to i}) \right], \quad (6)$$

where $\mathcal{S}(i)$ denotes the set of node i's intramodule nearest neighbors, and $\mathcal{F}(i)$ denotes the set of i's intermodule nearest neighbors. Note that products over empty sets $\mathcal{S}(i) = \emptyset$ or $\mathcal{F}(i) = \emptyset$ default to 1.

In practice, the message-passing equations are solved iteratively. Starting from a random initial configuration $\rho_{i\to j}, \varphi_{i\to j} \in \{0,1\}$, the messages are repeatedly updated until they finally converge. From the converged solutions for the messages, we can then compute the marginal probability $\rho_i = 0,1$ for each node i to belong to the giant connected activated component G:

$$\rho_i = \sigma_i \left[1 - \prod_{k\in\mathcal{S}(i)} (1-\rho_{k\to i}) \prod_{k\in\mathcal{F}(i)} (1-\varphi_{k\to i}) \right]. \quad (7)$$

The size of G, or rather the fraction of nodes belonging to G, can then simply be computed by summing the probability marginals ρ_i and dividing by the system size:

$$G(\vec{n}) = \frac{1}{N} \sum_{i=1}^{N} \rho_i. \quad (8)$$

IV. PERCOLATION PHASE DIAGRAM

In what follows, we derive an exact expression for the percolation threshold in Erdös-Rényi 2-NONs, defined as two

randomly interconnected ER modules. Each module is an ER random graph with Poisson degree distribution,

$$\mathbb{P}_z[k^{\text{conn}} = k] = e^{-z} z^k / k! \qquad \text{for } k \in \mathbb{N}_0, \tag{9}$$

where $z \equiv \langle k^{\text{conn}} \rangle$ denotes the average connectivity-degree. Similarly, we consider the inter-module links to form a bipartite ER random graph with Poisson degree distribution,

$$\mathbb{P}_w[k^{\text{ctr}} = k] = e^{-w} w^k / k! \qquad \text{for } k \in \mathbb{N}_0, \tag{10}$$

where $w \equiv \langle k^{\text{ctr}} \rangle$ denotes the average control-degree. The corresponding distributions for the connectivity- or control-degree of the node at the end of a randomly chosen intra- or interlink are given by

$$\begin{aligned} \mathbb{Q}_z[k^{\text{conn}} = k] &= k \mathbb{P}_z[k^{\text{conn}} = k]/z, \\ \mathbb{Q}_w[k^{\text{ctr}} = k] &= k \mathbb{P}_w[k^{\text{ctr}} = k]/w \end{aligned} \tag{11}$$

for $k \in \mathbb{N}^+$.

The random percolation process is then defined by removing each node in the NON independently with probability q, which is equivalently formulated as taking the configurations $\vec{n} = (n_1, \ldots, n_N)$ at random from the following product of Bernoulli distributions:

$$\mathbb{P}_p[\vec{n}] = \prod_{i=1}^{N} p^{n_i} (1-p)^{1-n_i}, \tag{12}$$

where $p = 1 - q$ denotes the occupation probability.

We thus take a slightly different yet mathematically equivalent perspective on the percolation process here: instead of randomly removing a fixed number qN of nodes, we consider configurations in which each node is independently removed with probability q. In the thermodynamic limit of large network size, both approaches are equivalent, as the distribution of configurations $\mathbb{P}_p[\vec{n}]$ is highly peaked around configurations $\vec{n}$ with qN removed nodes.

The probability $\mathbb{P}_p[\sigma_i = 1 | k_i^{\text{ctr}} = k]$ that a node with control-degree $k_i^{\text{ctr}} = k$ is activated when a randomly chosen fraction p of nodes in the NON is present can readily be obtained from the corresponding expectation $\langle \sigma_i \rangle_{\vec{n}}$, which is given by averaging the activation state σ_i in Eq. (1) over the distribution of configurations $\mathbb{P}_p[\vec{n}]$:

$$\langle \sigma_i \rangle_{\vec{n}} = p \, \mathbb{1}_{\{k_i^{\text{ctr}}=0\}} + p[1 - (1-p)^{k_i^{\text{ctr}}}] \mathbb{1}_{\{k_i^{\text{ctr}}>0\}}, \tag{13}$$

where $\mathbb{1}_{\{\cdot\}}$ denotes the indicator function. The expected fraction of activated nodes in the NON $\langle \sigma_i \rangle_{\vec{n}, k_i^{\text{ctr}}}$ is furthermore given by averaging $\langle \sigma_i \rangle_{\vec{n}}$ over the control-degree distribution $\mathbb{P}_w[k_i^{\text{ctr}} = k]$:

$$\langle \sigma_i \rangle_{\vec{n}, k_i^{\text{ctr}}} = p[1 + e^{-w} - e^{-wp}]. \tag{14}$$

Unlike a node's probability to be occupied, $\mathbb{P}_p[n_i = 1 | k_i^{\text{ctr}} = k] = \mathbb{P}_p[n_i = 1] = \langle n_i \rangle_{\vec{n}} = p$, the probability that a node with control-degree $k_i^{\text{ctr}} = k$ is activated,

$$\mathbb{P}_p[\sigma_i = 1 | k_i^{\text{ctr}} = k] = \begin{cases} p, & k = 0, \\ p[1 - (1-p)^k], & k > 0, \end{cases} \tag{15}$$

is therefore highly dependent on the node's control degree k_i^{ctr}. In other words, the deactivations ($\sigma_i = 1 \to \sigma_i = 0$) are highly degree-dependent, even if the fraction q of nodes to be removed from the NON ($n_i = 1 \to n_i = 0$) is chosen randomly.

To compute the expectation of messages within the ensemble of ER 2-NONs, we average the expressions for $\rho_{i \to j}$ and $\varphi_{i \to j}$, representing the converged solutions to the message-passing equations, over all possible realizations of randomness inherent in the above distributions (9)–(12). In doing so, however, we must make sure to properly account for the fact that, for nodes i with control links ($k_i^{\text{ctr}} \geqslant 1$), the binary occupation variable n_i shows up more than once within the entire system of message-passing equations, due to the activation rule for σ_i. Indeed, since the occupation variable is a binary number $n_i \in \{0,1\}$, powers of $n_i^k = n_i$ for each exponent $k \in \mathbb{N}^+$ and therefore the self-consistency is not affected by the existence of multiple n_i per node. Yet, when naively averaging with the distribution of configurations, we would incorrectly obtain $n_i^k \xrightarrow{\mathbb{P}_p} p^k$ instead of $n_i^k \xrightarrow{\mathbb{P}_p} p$, without properly accounting for the binary nature of the occupation variable across the entire system of message-passing equations.

More precisely, when inserting the expression for the message $\varphi_{k \to i}$, determined by Eq. (6), into the expression for $\rho_{i \to j}$, given by Eq. (5), the activation state $\sigma_k = n_k[1 - (1-n_i)\prod_{\ell \in \mathcal{F}(k) \setminus i}(1 - n_\ell)]$ (within $\varphi_{k \to i}$) reduces to n_k, since $n_i(1-n_i) = 0$ for binomial variables. In other words, we need to replace σ_k with n_k within the expression for $\varphi_{k \to i}$ [and analogously replace σ_i with n_i in Eq. (6)] when computing expectations.

Thus, the modified message-passing equations we need to average read

$$\begin{aligned} \rho_{i \to j} &= \sigma_i \left[1 - \prod_{k \in \mathcal{S}(i) \setminus j} (1 - \rho_{k \to i}) \prod_{k \in \mathcal{F}(i)} (1 - \varphi_{k \to i}) \right], \\ \varphi_{i \to j} &= n_i \left[1 - \prod_{k \in \mathcal{S}(i)} (1 - \rho_{k \to i}) \prod_{k \in \mathcal{F}(i) \setminus j} (1 - \varphi_{k \to i}) \right]. \end{aligned} \tag{16}$$

In practice, we expand $\rho_{i \to j}$, given by Eq. (16), and perform the averaging separately for each term:

$$\begin{aligned} \rho_{i \to j} = n_i &\left[1 - \prod_{k \in \mathcal{S}(i) \setminus j} (1 - \rho_{k \to i}) \right] \mathbb{1}_{\{k_i^{\text{ctr}}=0\}} \\ &+ \sigma_i \left[1 - \prod_{k \in \mathcal{S}(i) \setminus j} (1 - \rho_{k \to i}) \prod_{k \in \mathcal{F}(i)} (1 - \varphi_{k \to i}) \right] \mathbb{1}_{\{k_i^{\text{ctr}}>0\}}. \end{aligned} \tag{17}$$

The only nontrivial expectation involves the following expression:

$$\begin{aligned} &\left\langle \sigma_i \prod_{k \in \mathcal{S}(i) \setminus j} (1 - \rho_{k \to i}) \prod_{k \in \mathcal{F}(i)} (1 - \varphi_{k \to i}) \, \mathbb{1}_{\{k_i^{\text{ctr}}>0\}} \right\rangle \\ &\quad = \left\langle n_i \prod_{k \in \mathcal{S}(i) \setminus j} (1 - \rho_{k \to i}) \left[\prod_{k \in \mathcal{F}(i)} (1 - \varphi_{k \to i}) \right. \right. \\ &\qquad \left. \left. - \prod_{k \in \mathcal{F}(i)} (1 - n_k)(1 - \varphi_{k \to i}) \right] \mathbb{1}_{\{k_i^{\text{ctr}}>0\}} \right\rangle, \end{aligned} \tag{18}$$

where we have to account for the fact that $(1-n_k)(1-\varphi_{k\to i}) = (1-n_k)$. The final expression for the average intramodule message ρ reads

$$\rho = p[1 + e^{-w} - e^{-wp} - e^{-z\rho-w} + e^{-z\rho-wp} - e^{-z\rho-w\varphi}]. \tag{19}$$

Averaging the modified interlink message $\varphi_{i\to j}$, given by Eq. (16), over all possible realizations of randomness inherent in the percolation process yields

$$\varphi = p[1 - e^{-z\,\rho\,-w\,\varphi}]. \tag{20}$$

The percolation threshold $p_c = 1 - q_c$ of the ER 2-NON can now be found by evaluating the leading eigenvalue determining the stability of the fixed-point solution $\{\rho = \varphi = 0\}$ to the averaged modified message-passing equations [15]:

$$\begin{pmatrix} \frac{\partial\rho}{\partial\rho} & \frac{\partial\varphi}{\partial\rho} \\ \frac{\partial\rho}{\partial\varphi} & \frac{\partial\varphi}{\partial\varphi} \end{pmatrix}\Bigg|_{\{\rho=\varphi=0\}} = \begin{pmatrix} pz[1 + e^{-w} - e^{-wp}] & pz \\ pw & pw \end{pmatrix}. \tag{21}$$

The corresponding eigenvalues can readily be obtained as

$$\lambda_\pm = \frac{p}{2}\big[z[1+h] + w \pm \sqrt{z^2[1+h]^2 + 2zw[1-h] + w^2}\big], \tag{22}$$

where we define $h(p) \equiv e^{-w} - e^{-wp}$. Formally, the fixed-point solution $\{\rho = \varphi = 0\}$ is stable if and only if $\lambda_+ \leqslant 1$ [12,15]. The implicit function theorem then allows us to obtain the percolation threshold $p_c = 1 - q_c$ by saturating the stability condition as follows:

$$\lambda_+(p,z,w) = 1 \to p_c(z,w). \tag{23}$$

Results for $q_c(z,w) = 1 - p_c(z,w)$ in the ER 2-NON are shown in Fig. 3 and confirm the excellent agreement between direct simulations of the random percolation process on synthetic NONs and the theoretical percolation threshold calculated from Eq. (23). The numerically measured percolation thresholds, $q_c^{\rm num}(z,w)$, were obtained at the peak of the second largest activated component (Fig. 2), measured relative to the fraction of randomly removed nodes in the synthetic ER 2-NON. The analytical prediction of the percolation threshold, $q_c^{\rm analytic}(z,w)$, was obtained from the numerical solution of Eq. (23).

The large values of q_c in the percolation phase diagram confirm that the NON is very robust with respect to random node failures. The results indicate, for instance, that a fraction of more than 70% of randomly chosen nodes in an ER 2-NON with $\langle k^{\rm conn}\rangle = 4$ can be damaged without destroying the giant connected activated component G. Moreover, the percolation transition, separating the phases $G > 0$ and $G = 0$, is of second order in the robust NON (see Fig. 2).

Interestingly, the phase diagram reveals that, for a given average connectivity-degree z, the NON exhibits maximal vulnerability $q_c^{\rm min}(z,w^*) = 1 - p_c^{\rm max}(z,w^*)$ at a characteristic average control-degree $w^*(z)$, indicated by the dip in the percolation threshold q_c in Fig. 3. The equation determining $w^*(z)$ can straightforwardly be obtained via implicit differentiation of $\lambda_+(p_c,z,w) = 1$, using $\partial p_c/\partial w\,|_{w^*} = 0$. Explicitly, $w^*(z)$

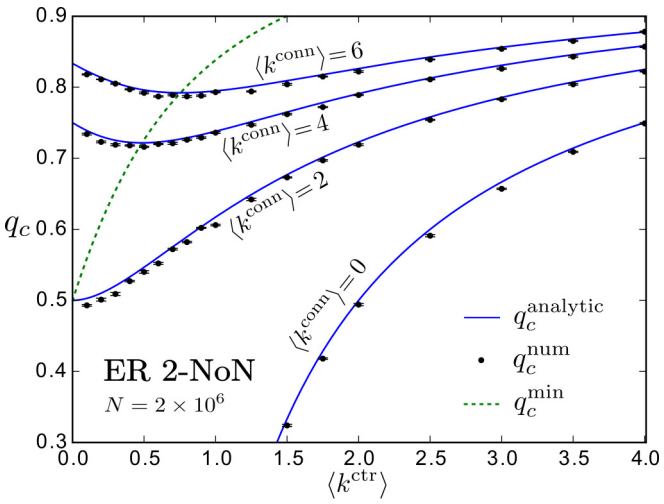

FIG. 3. Percolation phase diagram for ER 2-NONs. Blue curves show our analytical prediction of the percolation threshold, $q_c^{\rm analytic}$, as a function of $w \equiv \langle k^{\rm ctr}\rangle$ for different values of $z \equiv \langle k^{\rm conn}\rangle = 0,2,4,6$, obtained from Eq. (23). Black dots show the measured numerical percolation threshold, $q_c^{\rm num}$, from direct simulation of the random percolation process, obtained at the peak of the second largest connected activated component. The green dashed line indicates the maximal vulnerability $q_c^{\rm min}$ of the NON. Errors are standard errors of the mean (s.e.m.) over 10 NON realizations of system size $N = 2 \times 10^6$.

is determined by

$$\frac{p_c}{2}\left[1 + z\frac{\partial h}{\partial w} + \frac{z^2[1+h]\frac{\partial h}{\partial w} + z[1-h] - zw\frac{\partial h}{\partial w} + w}{\sqrt{z^2[1+h]^2 + 2zw[1-h] + w^2}}\right]\Bigg|_{w^*} = 0 \tag{24}$$

with $p_c(z,w)$ given by Eq. (23). The numerical solution for $w^*(z)$ is depicted in Fig. 4. The corresponding curve for $q_c^{\rm min}(z,w^*)$ is shown in Fig. 3 and can readily be seen to agree with the minimum of the analytical predictions $q_c^{\rm analytic}$ for the percolation thresholds.

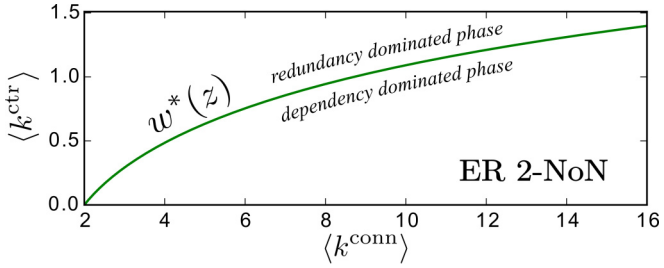

FIG. 4. Maximal vulnerability of ER 2-NONs. Critical average control degree $w^*(z) \equiv \langle k^{\rm ctr}\rangle^*(z)$ for which the ER 2-NON is most vulnerable, obtained from the solution of Eq. (24), for a given average connectivity degree $z \equiv \langle k^{\rm conn}\rangle$. $w^*(z)$ minimizes the critical fraction $q_c(z,w)$ of randomly removed nodes for which the giant activated component collapses, $G(q_c) = 0$, thereby marking the boundary above which an increase in the density of dependencies leads to a more robust NON. The corresponding curve for $q_c^{\rm min}$ is shown in Fig. 3.

Conceptually, the dip in q_c occurs as a consequence of the competition between dependency and redundancy effects in the NON. For $\langle k^{\rm ctr}\rangle < w^*$, the percolation threshold q_c, and therefore the robustness of the NON, decreases as the relative fraction of dependency links is increased. For $\langle k^{\rm ctr}\rangle > w^*$, however, the robustness of the NON increases again with increasing redundancy among the dependency connections. In other words, the critical average control-degree $w^*(z)$ marks the boundary above which the onset of redundancy reduces the impact of deactivations on the giant connected activated component G, and an increase in the density of dependencies therefore leads to a more robust NON.

The underlying mechanism responsible for the remarkable robustness of the NON is best understood from the behavior of the model in the limit $\langle k^{\rm conn}\rangle = 0$, which corresponds to a bipartite network equipped with our activation rule for σ_i, given by Eq. (1). The corresponding message-passing equations are straightforwardly obtainable from Eqs. (5) and (6), $\varphi_{i\to j} = \sigma_i[1 - \prod_{k\in\mathcal{F}(i)\setminus j}(1 - \varphi_{k\to i})]$, and can readily be seen to coincide with the usual single network message-passing equations by observing that σ_i can actually be replaced with n_i in this case [the reason is the following: assuming node i is present ($n_i = 1$), $\sigma_i = 0$ implies that none of i's intermodule neighbors is present and so none of the incoming intermodule messages can be nonzero either]. This property can of course directly be obtained also from Eq. (22), which in the limit $z = 0$ implies

$$\lambda_{\pm}^{z=0} = \frac{p}{2}\{\, w \pm \sqrt{w^2}\,\} \to p_c^{z=0} = 1/w. \qquad (25)$$

Therefore, the functioning of control links is well-defined even if they connect nodes that do not belong to the giant connected activated component. In the model of Refs. [2,3], on the other hand, dependency links only exist if they connect nodes that belong to the largest connected activated component in their own module. Hence, it is impossible to construct the NON from below p_c (or above q_c) using dependency links in the model of Refs. [2,3]. In the robust model, we can construct the links even if the nodes are not in G, allowing us to build the NON from below p_c using dependency connections. Thus, the transition is well-defined from above and below the percolation threshold.

V. MULTIPLEX NETWORKS

In this section, we show that our model of interdependencies as well as the presented approach to derive analytical expressions for the percolation phase diagram can straightforwardly be applied also to NON with replica nodes, also known as multiplex networks, multilayer networks or multigraphs [1,4]. A multiplex network consists of N nodes interconnected by different kinds of links, sometimes portrayed as a multilayer structure in which each layer is formed by a different type of links (connecting the same set of N nodes). Here we consider a multiplex network composed of two types of connections: connectivity and control links. More specifically, we consider Erdös-Rényi multiplex networks, where both layers are ER random graphs with Poisson degree distribution. Starting from a single ER random network with average degree $\langle k\rangle$, we randomly choose a fraction f of the edges and replace them with control links. We thus obtain

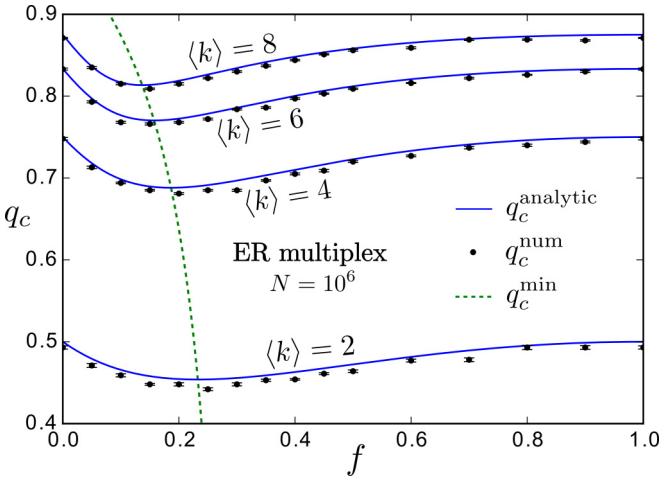

FIG. 5. Percolation phase diagram for ER multiplex networks composed of connectivity and control links. Blue curves show the analytical percolation thresholds, $q_c^{\rm analytic}$, as a function of the fraction of control links f for different values of $\langle k\rangle = \langle k^{\rm conn}\rangle + \langle k^{\rm ctr}\rangle = 2,4,6,8$, calculated from Eq. (23). Black dots show the measured numerical percolation thresholds, $q_c^{\rm num}$, from direct simulation of the random percolation process, obtained at the peak of the second largest connected activated component. The green dashed line indicates the maximal vulnerability $q_c^{\rm min}$ of the multiplex. Errors are s.e.m. over 10 realizations of system size $N = 10^6$.

an ER multiplex with average control-degree $w = f\langle k\rangle$ and average connectivity-degree $z = (1 - f)\langle k\rangle$, where the Poisson degree distributions are given by Eqs. (9) and (10).

The activation state σ_i of a node i in the multiplex is given by Eqs. (1) and (2), and the self-consistent system of message-passing equations, specifying for each node whether it belongs to the giant connected activated component G, can readily be seen to be given by Eqs. (5)–(7). Thus, the entire approach to derive the percolation phase diagram carries over, and indeed all of the above equations (1)–(25) are valid for ER multiplex networks as well.

The analytical and numerical results for the percolation phase transition $q_c(\langle k\rangle, f)$ in ER multiplex networks are shown in Fig. 5. The remarkable robustness of the network with respect to random node failures is again evident. Moreover, the phase diagram displays the same qualitative behavior with respect to the dip in $q_c(\langle k\rangle, f)$ as for the interdependent NON, which can again be understood to occur from the competition between dependency and redundancy effects in the network. The critical fraction of control dependencies $f^*(\langle k\rangle)$ for which the ER multiplex is most vulnerable and above which an increase in the fraction of control links results in a more robust network is shown in Fig. 6.

The percolation phase diagram for ER multiplex networks further illustrates the behavior of our model in the limit $f = 1$ (corresponding to the limit $z = 0$ discussed above), where the network is formed entirely from control links. The limit $f = 1$ can readily be seen to coincide with the usual single network limit $f = 0$, where the network is formed entirely from connectivity links.

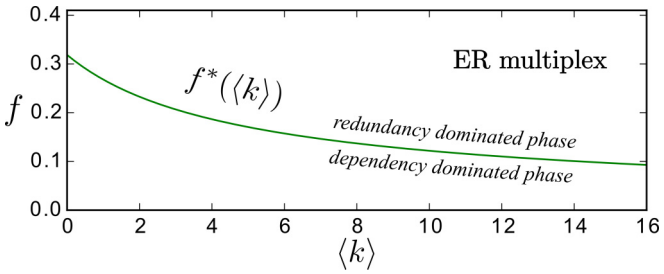

FIG. 6. Maximal vulnerability of ER multiplex. Critical fraction of control links $f^*(\langle k\rangle)$ for which the ER multiplex is most vulnerable, obtained from the solution of Eq. (24), for a given average degree $\langle k\rangle = \langle k^{\text{conn}}\rangle + \langle k^{\text{ctr}}\rangle$. $f^*(\langle k\rangle)$ minimizes the percolation threshold $q_c(\langle k\rangle, f)$ of randomly removed nodes for which the giant connected activated component collapses, $G(q_c) = 0$, thus marking the boundary above which an increase in the fraction of control dependencies results in a more robust network. The corresponding curve for $q_c^{\min}$ is shown in Fig. 5.

VI. CONCLUSION

In conclusion, we have seen that the robustness in NONs can be understood to emerge if dependency or control links do not need to be part of the giant connected activated component G for their proper functioning. In contrast to previously existing models of interdependent networks [2,3], dependencies in the robust NON do not lead to cascades of failures. The key point in our model is that a node can be activated even if it does not belong to G. An example of the structure of a NON where the model applies is that of the brain [6–10]. While in Ref. [6] we have shown that the model of [2] becomes robust when correlations in the dependencies are considered, here we show that a local activation rule Eq. (1) akin to brain control between modules defines a novel model of a NON that is robust even without correlations. We have seen that the maximal vulnerability of the NON occurs as a consequence of the competition between dependency and redundancy effects, where the critical fraction of dependencies marks the boundary above which the robustness of the system improves with increasing control or dependency connections. We have shown that our model of interdependencies can readily be applied also to multiplex networks. The presented framework allows us to derive analytical expressions for the percolation phase diagram of interdependent networks with arbitrary degree distributions, for which theoretical predictions similar to the ones presented can be obtained. Our model is straightforwardly generalizable also to directed links.

ACKNOWLEDGMENTS

Research reported in this publication was supported by the National Cancer Institute of the National Institutes of Health under Awards No. U54CA137788/U54CA132378 and No. NIH-NIBIB 1R01EB022720-01, NSF PHY-1305476, NSF-IIS 1515022, and Army Research Laboratory Cooperative Agreement No. W911NF-09-2-0053 (the ARL Network Science CTA).

[1] M. E. J. Newman, *Networks: An Introduction* (Oxford University Press, New York, 2010).
[2] S. V. Buldyrev, R. Parshani, G. Paul, H. E. Stanley, and S. Havlin, Nature (London) **464**, 1025 (2010).
[3] J. Gao, S. V. Buldyrev, H. E. Stanley, and S. Havlin, Nat. Phys. **8**, 40 (2012).
[4] G. Bianconi, S. N. Dorogovtsev, and J. F. F. Mendes, Phys. Rev. E **91**, 012804 (2015).
[5] R. Parshani, S. V. Buldyrev, and S. Havlin, Phys. Rev. Lett. **105**, 048701 (2010).
[6] S. D. S. Reis, Y. Hu, A. Babino, J. S. Andrade Jr., S. Canals, M. Sigman, and H. A. Makse, Nat. Phys. **10**, 762 (2014).
[7] F. Morone, K. Roth, B. Min, H. E. Stanley, and H. A. Makse, Proc. Natl. Acad. Sci. (USA) **114**, 3849 (2017).
[8] L. K. Gallos, H. A. Makse, and M. Sigman, Proc. Natl. Acad. Sci. (USA) **109**, 2825 (2012).
[9] L. K. Gallos, M. Sigman, and H. A. Makse, Front. Physiol. **3**, 123 (2012).
[10] C. D. Gilbert and M. Sigman, Neuron **54**, 677 (2007).
[11] X. Yuan, Y. Hu, H. E. Stanley, and S. Havlin, Proc. Natl. Acad. Sci. (USA) **114**, 3311 (2017).
[12] F. Morone and H. A. Makse, Nature (London) **524**, 65 (2015).
[13] F. Morone, B. Min, L. Bo, R. Mari, and H. A. Makse, Sci. Rep. **6**, 30062 (2016).
[14] W. S. McCulloch and A. Pitts, Bull. Math. Biophys. **5**, 115 (1943).
[15] B. Karrer, M. E. J. Newman, and L. Zdeborová, Phys. Rev. Lett. **113**, 208702 (2014).
[16] S. N. Dorogovtsev, J. F. F. Mendes, and A. N. Samukhin, Nucl. Phys. B **653**, 307 (2003).
[17] M. Mézard and A. Montanari, *Information, Physics, and Computation* (Oxford University Press, New York, 2009).